Correlation-Aware QoS Routing With Differential Coding for Wireless Video Sensor Networks

Rui Dai, *Student Member, IEEE*, Pu Wang, *Student Member, IEEE*, and Ian F. Akyildiz, *Fellow, IEEE*

***Abstract*—The spatial correlation of visual information retrieved from distributed camera sensors leads to considerable data redundancy in wireless video sensor networks, resulting in significant performance degradation in energy efficiency and quality-of-service (QoS) satisfaction. In this paper, a correlation-aware QoS routing algorithm (CAQR) is proposed to efficiently deliver visual information under QoS constraints by exploiting the correlation of visual information observed by different camera sensors. First, a correlation-aware inter-node differential coding scheme is designed to reduce the amount of traffic in the network. Then, a correlation-aware load balancing scheme is proposed to prevent network congestion by splitting the correlated flows that cannot be reduced to different paths. Finally, the correlation-aware schemes are integrated into an optimization QoS routing framework with an objective to minimize energy consumption subject to delay and reliability constraints. Simulation results demonstrate that the proposed routing algorithm achieves efficient delivery of visual information under QoS constraints in wireless video sensor networks.**

***Index Terms*—Quality-of-service (QoS), routing, spatial correlation, video compression, wireless video sensor networks.**

I. Introduction

RECENT advances in imaging hardware and wireless communications have fostered the use of video sensors in various distributed sensing applications [10], [16]. By integrating imaging sensor, embedded processor, memory, and wireless transceivers on a single device, a video sensor node is able to retrieve, process, store, and transmit visual information under limited power supply. Networks of interconnected video sensor nodes are referred to as wireless video sensor networks (WVSNs) [2], [24], in which multiple video sensors collaborate with each other to provide enriched observations of the environment. WVSNs can enhance a lot of applications such as environmental monitoring, traffic enforcement, and remote health care. Most of these applications require that visual information be delivered under predefined quality-of-service (QoS) constraints. This is a challenging task because video sensors are constrained in battery and processing capabilities, while the delivery of visual information is resource-demanding.

Manuscript received March 02, 2011; revised August 30, 2011 and November 27, 2011; accepted March 16, 2012. Date of publication April 26, 2012; date of current version September 12, 2012. This work was supported by the U.S. National Science Foundation (NSF) under Grant No. ECCS-0701559. The associate editor coordinating the review of this manuscript and approving it for publication was Dr. Zhihai (Henry) He.

The authors are with the Broadband Wireless Networking Laboratory, School of Electrical and Computer Engineering, Georgia Institute of Technology, Atlanta, GA 30332 USA (e-mail: rui.dai@gatech.edu; pwang40@ece.gatech.edu; ian@ece.gatech.edu).

Color versions of one or more of the figures in this paper are available online at http://ieeexplore.ieee.org.

Digital Object Identifier 10.1109/TMM.2012.2194992

Many recent works have been proposed for providing QoS support at different layers of the communication stack, including QoS routing algorithms [9], QoS MAC protocols [19], and cross-layer QoS solutions [21]. These works, however, only try to meet QoS requirements by properly regulating the network traffic, while the total amount of data injected into the network cannot be reduced. Therefore, It is still resource-demanding to deliver large amounts of visual information in WVSNs. To encounter this problem, collaborative multimedia in-network processing [2] is suggested to reduce the traffic volume by allowing sensor nodes to filter out uninteresting events locally or coordinate with each other to aggregate correlated data. In WVSNs, correlation exists among the observations of video sensors with overlapped field of views (FoVs) [6], leading to considerable data redundancy. It is highly desirable to remove such redundancy to improve the performance of WVSNs [2].

To enhance energy efficiency, the joint compression/aggregation and routing approach has been studied for sensor networks that deal with scalar data. This approach can be classified into three categories [22]: distributed source coding (DSC), routing driven compression (RDC), and compression driven routing (CDR). DSC aims to allocate the optimal coding rates to minimize the total communication cost of transporting correlated information over shortest paths. In RDC, sensors send data along the preferred paths to the sink while allowing for opportunistic aggregation wherever the paths overlap. In contrast, CDR let nodes select the paths that allow for the maximum possible aggregation at each hop. These works cannot provide QoS supports such as *timeliness* and *reliability*, and thus are not applicable to WVSNs.

In this paper, we propose a correlation-aware QoS routing algorithm (CAQR) for the efficient delivery of visual information in WVSNs. First, based on the spatial correlation of visual information in our previous work [6], a correlation-aware inter-node differential coding scheme is proposed to reduce the amount of traffic in the network, where differential coding is performed between intra coded frames generated by correlated sensors. Then, a correlation-aware load balancing scheme is proposed to prevent network congestion by splitting the correlated flows that cannot be reduced to different paths. By integrating these correlation-aware schemes, an optimization QoS routing framework is proposed with an objective to minimize sensors' energy consumption under delay and reliability constraints. It is shown that by integrating the corrrelation-aware schemes, the proposed algorithm can achieve energy efficient QoS communication in WVSNs.

II. Related Work

Joint compression/aggregation and routing has been proposed to deal with scalar data in sensor networks. In [22], the

performances of different routing with compression schemes are analyzed. The problem of correlated data gathering is studied in [5] and [18], where the goal is to minimize the total communication cost in the network. The Minimum Fusion Steiner Tree (MFST) routing algorithm [20] is proposed for energy efficient data gathering with aggregation, in which both costs for data transmission and data fusion are optimized. Although these results work well for scalar data, new solutions are needed for the delivery of visual information which has high bandwidth demand and QoS requirements.

Most QoS routing protocols for wireless sensor networks are designed to support two performance metrics: *timeliness* and *reliability*. The SPEED [13] protocol achieves end-to-end soft real-time communication by maintaining a desired delivery speed across the sensor network through nondeterministic geographic forwarding. While SPEED does not consider energy consumption, a real-time power-aware routing protocol (RPAR) [4] is designed that dynamically adjusts transmission power and routing decisions to meet the packet deadlines. An extension of the SPEED protocol, the MMSPEED [9] provides probabilistic reliability guarantee through multipath forwarding. To support the high data rate traffic of video sensors, the directional geographical routing algorithm (DGR) [3] constructs multiple disjoint paths for a video sensor by adjusting the deviation angle at each hop, and the data from a video sensor is split and forwarded through these disjoint paths. These solutions only try to provide QoS guarantee by properly distributing network traffic, and it is still resource-demanding to deliver intensive visual information in WVSNs.

III. Correlation of Visual Information

In a densely deployed WVSN, there exists correlation among the observations from video sensors with overlapped FoV. We first study the correlation characteristics of visual information in WVSNs, and then discuss video in-network compression mechanisms for reducing traffic redundancy.

A. Correlation of Visual Information in Sensor Networks

A video sensor can only observe the objects within its FoV. As shown in Fig. 1(a), the FoV of a video sensor is determined by four parameters: the location of the video sensor (P), the sensing radius (R), the sensing direction $(\vec{V})$, and the offset angle (α). The sensing process of a video sensor is characterized by projection from a 3-D scene to a 2-D image, for which the key parameter is the sensor's focal length (f). To simplify the problem, we consider the case that all the video sensors in a network are homogeneous (i.e., they share the same values of f, R, and α). For two sensors V_A and V_B with FoVs F_A and F_B, suppose at a same time, their observed images are X_A and X_B, respectively. X_A and X_B are correlated if F_A and F_B are overlapped with each other. We introduce two metrics to characterize the correlation between video sensors.

1) Overlapped Ratio of FoVs: The overlapped ratio of FoVs for V_A and V_B, denoted by r_{AB}, is defined as

$$r_{AB} = \frac{S(F_{AB})}{S(F_A)} \tag{1}$$

where $S(F_{AB})(F_{AB} = F_A \cap F_B)$ is the overlapped area of F_A and F_B [Fig. 1(b)], and $S(F_A)$ is the area of F_A. If two video sensors have large overlapped ratio of FoVs, large portions of the two observed images are correlated, and they are likely to observe the same event concurrently.

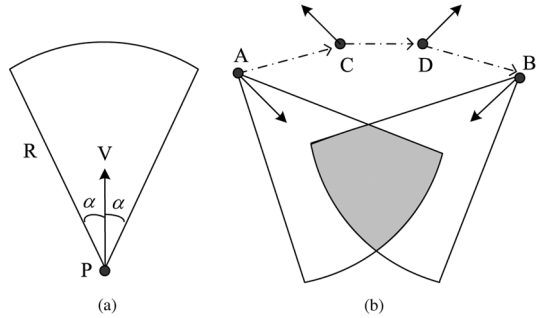

Fig. 1. (a) FoV. (b) Overlapped FoVs.

2) Spatial Correlation Coefficient: We also use the spatial correlation coefficient in our previous work [6], [27]. If two video sensors V_A and V_B can both observe an area of interest F_{AB}, a spatial correlation coefficient ρ_{AB} was derived as a function of the positions (P_A, P_B) and sensing directions $(\vec{V_A}, \vec{V_B})$ of the two sensors and the overlapped FoV (F_{AB}):

$$\rho_{AB} = f(P_A, \vec{V_A}, P_B, \vec{V_B}, F_{AB}). \tag{2}$$

This is a normalized metric ranging from 0 to 1 and it indicates the degree of correlation between the two sensors.

One promising property of the spatial correlation coefficient is its capability of estimating the coding efficiency among correlated video sensors. Consider two correlated images (X_A and X_B) from sensors V_A and V_B. Each sensor can compress/encode its observed image independently, and we denote the resulting coding rates by $R(X_A)$ and $R(X_B)$. Since X_A and X_B are correlated, we can take X_B as a reference image, and compress X_A using X_B as its prediction. This is referred to as differential coding or predictive coding. For spatially correlated frames, differential coding could be achieved through inter-frame prediction such as motion estimation or disparity compensation [25] in H.264/AVC. Suppose the rate of X_A becomes $R(X_A|X_B)$ after differential coding. We define a *differential coding efficiency* as the percentage of rate saved by differential coding compared to individual coding:

$$\eta = \frac{R(X_A) - R(X_A|X_B)}{R(X_A)}. \tag{3}$$

As entropy is the lower bound for coding rate, an estimation of the differential coding efficiency can be obtained from the entropies of the image sources. We define an *estimated differential coding efficiency* as

$$\eta_H = \frac{H(X_A) - H(X_A|X_B)}{H(X_A)} = \frac{I(X_A; X_B)}{H(X_A)} \tag{4}$$

where $I(A; B)$ is the mutual information between X_A and X_B. It is shown in our previous work [6], [27] that $I(A; B)$ is proportional to both the overlapped ratio of FoVs (r_{AB}) and the spatial correlation coefficient (ρ_{AB}). We consider the case that the individual entropies are the same for all sensor nodes $(H(X_A) = H(X_B))$. Consequently, η_H is proportional to both r_{AB} and ρ_{AB}, and η_H will be high when both r_{AB} and ρ_{AB} are large.

3) Costs for Estimating Correlation: To estimate the overlapped ratio of FoVs (1), we just need the four FoV parameters [P, R, $\vec{V}$, and α in Fig. 1(a)]. The correlation coefficient in (2) could also be easily calculated from the FoV parameters and focal lengths of cameras as shown in [6]. With the correlation coefficient, the differential coding efficiency (4) is easily calculated as shown in [27]. Both the FoV parameters and the focal lengths could be estimated through calibration methods for distributed camera networks, such as [7]. In most cases, the video sensors stay still, so the estimation of correlation metrics just needs to be performed during network deployment. When a sensor changes its position or new sensors are added to the network, the correlation metrics can be updated by exchanging a few parameters. Estimating the correlation metrics does not require expensive communication or computation resources.

B. Video In-Network Compression

Due to the huge size of raw visual information, images and video sequences are compressed prior to transmission. A lot of standardized techniques can be applied for image and video coding, such as JPEG/JPEG 2000 and H.26x/MPEG. These standards are based on the predictive coding concept. In contrast, distributed video coding (DVC) [11] allows for separate encoding of correlated sources and joint decoding at the end user. DVC is introduced to reduce the computational complexity at the encoders, however, there is a lack of practical implementations of DVC in sensor networks. On the other hand, there are many studies on reducing the computational complexity on low-power DSPs for standardized coding techniques. For these reasons, we consider the standardized coding techniques in our work.

Standardized coding techniques can be classified into intra coding and inter coding. Intra coding reduces the redundancy within an image, while inter coding (also called differential or predictive coding) reduces the redundancy among multiple images. Accordingly, a compressed video sequence usually consists of periodical intra coded reference (I) frames and inter coded frames between reference frames. Inter coding has much higher coding efficiency than intra coding, consequently, intra coded frames have much larger sizes than inter coded frames. Intra frames are introduced periodically to reduce the propagation of packet losses/errors or to start an independent piece of video stream.

In a WVSN, correlated video sensors can cooperate with each other and remove the redundancy among their observations. We can perform differential coding on the intra coded (I) frames between correlated sensors. Since video sensors that are out of the communication ranges of each other can still observe a common scene [24] [Fig. 1(b)], the coding between correlated sensors could be integrated in the network layer operations. Accordingly, flows generated by video sensors could be classified into two categories:

1) *Intra flows*: Flows of intra coded video frames. The amount of traffic for an intra flow might be further reduced by differential coding among correlated sensors.
2) *Inter flows*: Flows of inter coded video frames, for which the amount of traffic can hardly be further reduced.

Both types of flows need to be forwarded to the sink efficiently under QoS constraints.

C. Energy Consumption Models

The energy consumption for both video communication and processing are not negligible. We first consider a one-hop communication case. Suppose one sensor node transmits l bits of data over a distance d to another node. The energy consumption for transmission is

$$E(l,d)_{\text{trans}} = E_{\text{elec}} \cdot l + \varepsilon_{\text{amp}} \cdot d_{\text{hop}}^{\alpha} \cdot l \tag{5}$$

while the energy consumption for receiving these l bits is

$$E(l,d)_{\text{recv}} = E_{\text{elec}} \cdot l \tag{6}$$

where E_{elec} is the energy needed by the transceiver circuitry to transmit or receive one bit, ε_{amp} is a constant for communication energy, and α is the path loss exponent. The total energy consumption for transmitting and receiving l bits over a distance d is given by

$$E(l,d) = 2 \cdot E_{\text{elec}} \cdot l + \varepsilon_{\text{amp}} \cdot d_{\text{hop}}^{\alpha} \cdot l. \tag{7}$$

The energy consumption for processing can be modeled as a function of supply voltage. Suppose the execution of a task consisting of N_{cyc} clock cycles, the energy consumption for processing is estimated as

$$E_{\text{proc}}(N) = N_{\text{cyc}} C_{\text{total}} V_{dd}^2 + V_{dd} \left(I_0 e^{\frac{V_{dd}}{nV_T}} \right) \left(\frac{N_{\text{cyc}}}{f} \right). \tag{8}$$

The first term in (8) is the switching energy, where C_{total} is the total capacitance switched by the computation per cycle, and V_{dd} is the supply voltage. The second term stands for the leakage energy, where f is the clock speed, and I_0, n, K, and c are processor-dependent parameters [26].

The processing burden in WVSNs mainly comes from the video encoding and decoding process. The computational complexity of standardized video codecs has been studied a lot in the literature. From the experimental results in [12] and [14], the number of clock cycles for encoding or decoding a video frame could be estimated. Together with the processor-dependent parameters in (8), we can estimate the energy consumption for encoding and decoding video frames.

IV. Correlation-Aware QoS Routing

We propose a correlation-aware QoS routing algorithm (CAQR) for the delivery of visual information in WVSNs. By utilizing the correlation characteristics of video sensors, the algorithm achieves energy-efficient delivery of visual information while satisfying QoS constraints. CAQR is a distributed routing solution for WVSNs, and its components are designed to be implemented on each sensor node. In the following, we explain the CAQR algorithm in detail.

A. Correlation Groups Construction

According to the analysis in Section III, video sensors with large overlapped FoVs are likely to report the same event concurrently, and they are likely to have high differential coding gains. We introduce a centralized preprocessing step to cluster

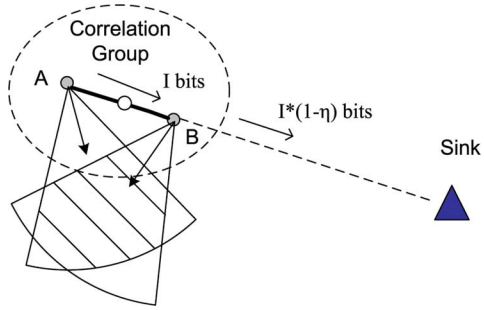

Fig. 2. Correlation-aware differential coding.

video sensors with large overlapped FoVs into *correlation groups*.

Let each video sensor report its focal length and FoV parameters to the sink. After receiving these parameters, the sink calculates the overlapped ratio of FoVs (r) (1) between any two video sensors. We apply the hierarchical clustering algorithm in [15]. By using the overlapped ratio of FoVs (r_{ij}) as a similarity metric, the hierarchical clustering algorithm groups sensors with large overlapped ratio of FoVs together. After running the clustering algorithm, the sink broadcasts the results of clustering and assigns a group ID for each group. Each video sensor will be notified its group ID and other sensors' sensing parameters in the same correlation group. The construction of correlation groups just need to be performed once while deploying the network. In the following steps of the routing algorithm, correlation-aware operations are performed among video sensors that belong to the same correlation groups.

B. Intermediate Node Selection for Correlation-Aware Differential Coding

We introduce a correlation-aware inter-node differential coding scheme for the routing of intra flows. As shown in Fig. 2, sensor V_A needs to find a route for its intra frame X_A to the sink. It could find another candidate sensor in the same group that is closer to the sink to perform differential coding. Suppose sensor V_B is in the same group as V_A and its distance to the sink is closer than $V_A (d_{BS} < d_{AS})$. From our correlation model, we can estimate the differential coding efficiency η_{AB} in (4). If the size of the intra frame X_A is I_A, the saved bits from differential coding can be estimated as $I_A \cdot \eta_{AB}$. We introduce an energy gain to evaluate the potential energy efficiency of differential coding between V_A and V_B:

$$G_E(V_A, V_B) = \frac{E_{\text{com}}\{I_A \cdot \eta_{AB}\}}{E_{\text{proc}}\{I_A\}}. \tag{9}$$

The numerator in the gain function is the communication energy for the bits that are saved from differential coding. It stands for the benefits brought by differential coding. This communication energy is not only related to the number of saved bits, but also related to the distance and number of hops from sensor V_B to the sink. We can estimate E_{com} using the estimated number of hops from node V_B to the sink $(\hat{N}_B^{\text{hops}})$ and the average one-hop distance (d_{hop}), given by

$$E_{\text{com}}\{I_A \cdot \eta_{AB}\} = \hat{N}_B^{\text{hops}} \cdot E(I_A \cdot \eta_{AB}, d_{\text{hop}}) \tag{10}$$

where $E(I_A \cdot \eta_{AB}, d_{\text{hop}})$ is obtained from (7) and $\hat{N}_B^{\text{hops}}$ can be estimated by

$$\hat{N}_B^{\text{hops}} = \max\left(\left\lceil \frac{d_{BS}}{d_{\text{hop}}} \right\rceil, 1\right). \tag{11}$$

To estimate the average one-hop distance between nodes in the network (d_{hop}), node V_A can acquire all its one-hop neighbors' positions through a few message exchanges. Also d_{hop} could be estimated as the sample arithmetic mean of the distance between V_A and all its one-hop neighbors. This estimation method involves little cost. It will be representative if the density of sensors are similar across the whole network.

The denominator in (9) is the energy costs for performing differential coding, i.e., the processing energy of differential coding at sensor V_B, including the decoding of the intra frame and the differential coding of the intra frame X_A with respect to the frame X_B at V_B. The energy for processing is related to video frame size and hardware. This term could be estimated from (8) using the parameters in [12] and [14].

For the routing of an intra frame generated at node V_A in correlation group $\mathcal{G}(V_A)$, we intend to find the best intermediate node in the same group so that the energy gain is maximized. This problem can be formulated as follows.

Differential coding-based intermediate node selection (DCIS)

$$\text{Find: } V_{B^*} = \arg \max_{V_B \in \mathcal{G}(V_A)} G_E(V_A, V_B) \tag{12}$$

$$\text{Subject to: } d_{BS} < d_{AS}, : G_E(V_A, V_B) > 1. \tag{13}$$

A node V_B for differential coding should satisfy two conditions: 1) V_B is closer to the sink than V_A, which is given as $d_{BS} < d_{AS}$; 2) the energy gain for differential coding is larger than 1. Among all the nodes in group $\mathcal{G}(V_A)$ that satisfy these two conditions, the node that generates the maximum energy gain (V_{B^*}) is selected as the intermediate node.

After V_A determines V_{B^*} for differential coding, it sends a request message to V_{B^*}, and V_{B^*} will send back a reply message. In this way, V_{B^*} becomes an intermediate destination for the intra frames generated by V_A. The intra frames from V_A will be forwarded to V_{B^*} first; V_{B^*} will further compress the frame and then forward it to the sink.

C. QoS Guaranteed Next-Hop Selection

Each node distributively select the optimal next-hop with the objective of minimizing energy consumption and satisfying QoS requirements in delay and reliability. Table I lists the relevant notations and variables for this algorithm.

Suppose node i needs to forward a video frame to the destination $\mathcal{D}$. ($\mathcal{D}$ can be either an intermediate node for differential coding or the sink.) We define the forwarding neighbor set of node i as a set of its neighbors that are closer to the sink than itself, denoted by $\mathcal{F}_i$. The next hop node is selected from $\mathcal{F}_i$ according to the following rules.

Distributed correlation-aware QoS routing (DCR)

$$\text{Given } : i, \mathcal{D}, j \in \mathcal{F}_i, V_{id}, \mathcal{G}(V_{id}), \{R_0^C, \ldots, R_N^C\}$$

$$\text{Find } : j^*, R_{ij^*}^C \tag{14}$$

$$\text{Minimize } : E(L/R_{ij}^C, d_{ij}) \tag{15}$$

TABLE I
NOTATIONS AND VARIABLES

$\mathcal{F}_i$	forwarding neighbor set of node i	$\mathcal{D}$	destination of a route
V_{id}	ID of a video sensor	$\mathcal{G}(V_{id})$	correlation group of sensor V_{id}
L	packet length	d_{ij}	distance between node i and node j
$\{R_0^C, \ldots, R_N^C\}$	candidate channel coding rates	R_{ij}^C	channel coding rate for link ij
R	transmission rate	T_{ij}	local delay constraint
t_{ij}^q	local queueing delay	PR_{ij}	required local packet delivery ratio
pr_{ij}	local packet delivery ratio	x_{v^j}	correlation group indicator
DT	frame decodable threshold (%)	φ	probability that DT packets are delivered
$P_{\mathcal{D}}$	probability that a frame is decoded	p_b	bit error rate

$$\text{Subject to } : \frac{L}{R \cdot R_{ij}^C} + \overline{t_{ij}^q} < T_{ij} \tag{16}$$

$$\frac{\gamma}{1-\gamma}\left(\Delta t_{ij}^q\right)^2 \le \left(T_{ij} - \frac{L}{R \cdot R_{ij}^C} - \overline{t_{ij}^q}\right)^2 \tag{17}$$

$$\mathrm{pr}_{ij} \ge \mathrm{PR}_{ij} \tag{18}$$

$$\sum_{v^j \in \mathcal{L}\{v^j\}} x_{v^j} < w. \tag{19}$$

The locally optimal next hop j^* is the node that results in the minimum energy consumption under local delay, local reliability, and correlation-aware load balancing requirements. A channel coding rate for the link from i to j^*, $R_{ij^*}^C$, is also selected from a set of predefined rates $\{R_0^C, \ldots, R_N^C\}$.

The objective is to minimize energy consumption. As shown in (15), the minimization term is the energy consumption for transmitting a packet of L bits data and header with channel coding rate R_{ij}^C over a distance of d_{ij}. Equations (16) and (17) are the local delay requirements, (18) is the local reliability requirement, and (19) is the constraint for correlation-aware load balancing.

1) Local Delay Requirements: We use a geographic based mechanism to map end-to-end delay requirements to local delay requirements. Suppose a video flow v at node i needs to be delivered to the destination $\mathcal{D}$ within time $T_{i\mathcal{D}}$. The local delay constraint, T_{ij}, is given as

$$T_{ij} = \left(\frac{d_{i\mathcal{D}} - d_{j\mathcal{D}}}{d_{i\mathcal{D}}}\right) \cdot T_{i\mathcal{D}} \tag{20}$$

where $d_{i\mathcal{D}}$ is the distance from node i to the destination, and $d_{j\mathcal{D}}$ is the distance from node j to the destination.

We consider a contention-free MAC in our context. Under this assumption, the delay of a hop mainly consists of the transmission delay and the queueing delay. The transmission delay for a packet from node i to node j can be calculated as $(L)/(R \cdot R_{ij})$, where L is the length of the packet, R is the transmission rate, and R_{ij}^C the channel coding rate. We denote the queueing delay from node i to j by t_{ij}^q. Then the total delay from node i to j is given by $(L)/(R \cdot R_{ij}) + t_{ij}^q$.

We provide probabilistic guarantee for one-hop delay, in which the probability that a packet is delivered within deadline should not be below γ, given by $P((L)/(R \cdot R_{ij}^C) + t_{ij}^q \le T_{ij}) \ge \gamma$. It can also be expressed as

$$P\left(\frac{L}{R \cdot R_{ij}^C} + t_{ij}^q \ge T_{ij}\right) \le 1 - \gamma. \tag{21}$$

We let node j maintain the delays of packets in a recent period, from which we can estimate the average queueing delay $\overline{t_{ij}^q}$ and the variance of queueing delay $(\Delta t_{ij}^q)^2$. As a result, the average single hop delay is $(L)/(R \cdot R_{ij}^C) + \overline{t_{ij}^q}$, while the variance of single hop delay is $(\Delta t_{ij}^q)^2$.

According to one-sided Chebyshev's inequality, for a random variable X with mean μ and variance σ^2, it satisfies

$$P(X - \mu \ge k) \le \frac{\sigma^2}{\sigma^2 + k^2}, k > 0. \tag{22}$$

By applying the Chebyshev's inequality on (21), we find

$$P\left(\frac{L}{R \cdot R_{ij}^C} + t_{ij}^q \ge T_{ij}\right) \le \frac{\left(\Delta t_{ij}^q\right)^2}{\left(\Delta t_{ij}^q\right)^2 + \left(T_{ij} - \frac{L}{R \cdot R_{ij}} - \overline{t_{ij}^q}\right)^2} \tag{23}$$

and

$$T_{ij} - \left(\frac{L}{R \cdot R_{ij}^C} + \overline{t_{ij}^q}\right) > 0. \tag{24}$$

Based on (23) and (24), we have derived two constraints to satisfy the probabilistic delay guarantee in (21), which are given in (16) and (17). Condition (24) corresponds to constraint (16). Comparing (23) and (21), if the condition

$$\frac{\left(\Delta t_{ij}^q\right)^2}{\left(\Delta t_{ij}^q\right)^2 + \left(T_{ij} - \frac{L}{R \cdot R_{ij}} - t_{ij}^q\right)^2} \le 1 - \gamma \tag{25}$$

is met, the probabilistic delay guarantee inequation (21) could be satisfied, from which constraint (17) is obtained.

2) Local Reliability Requirements: We incorporate a *dynamic channel coding* scheme in the routing algorithm to adapt to varying wireless channel conditions. The routing algorithm selects a proper channel coding rate for link i to j, R_{ij}^C, from a set of predefined channel coding rates $\{R_0^C, \ldots, R_N^C\}$. A smaller channel coding rate indicates more redundancy being added to a packet and better error resilience performance.

To evaluate reliability, we use *packet delivery ratio*, the percentage of packets successfully delivered to the destination. If we require that each hop on a route should provide the same level of reliability, the required packet delivery ratio from node i to node j, PR_{ij}, can be estimated as

$$\mathrm{PR}_{ij} = \mathrm{PR}^{1/\hat{N}_{ij}} \tag{26}$$

where PR is the required packet delivery ratio given by the applications, and $\hat{N}_{ij}$ is the estimated number hops from i to the destination if j is selected as its next hop, i.e.,

$$\hat{N}_{ij} = \max\left(\left\lceil \frac{d_{i\mathcal{D}}}{\hat{d_{ij}}} \right\rceil, 1\right) \tag{27}$$

where $\hat{d_{ij}}$ is the projection of d_{ij} onto the line connecting node i with the sink.

Now we explain how to obtain the required packet delivery ratio PR. An end-to-end video application usually cares if a video frame can be successfully decoded or not. Therefore, we use the *probability that a video frame is successfully decoded* [28] as a metric to evaluate reliability. We denote this probability by P_D. A video frame X is packed into n packets for transmission. The frame will be decodable only when enough packets are received correctly. We introduce *frame decodable threshold* [28], denoted by DT, to represent the percentage of packets needed to decode a frame. This threshold is dependent on specific video coders and their error recovering capabilities. Let PR be the packet delivery ratio of each packet. The probability that at least DT percent of the packets are successfully delivered, denoted by $\varphi(X)$, is estimated from n, DT, and PR, given by

$$\begin{aligned}\varphi(X) &= \varphi(n, \mathrm{DT}, \mathrm{PR}) \\ &= \sum_{i=\lceil n\cdot \mathrm{DT}\rceil}^{n} \binom{n}{i} \cdot \mathrm{PR}^i \cdot (1-\mathrm{PR})^{n-i}. \end{aligned} \quad (28)$$

An intra coded frame is decodable if at least DT percent of the packets are delivered to the sink, e.g., if a video sensor V_A has generated an intra frame X_A. The probability that X_A is successfully decoded is given as

$$P_D(X_A) = \varphi(X_A) = \varphi(n_A, \mathrm{DT}, \mathrm{PR}_A) \quad (29)$$

where n_A is the number of packets for X_A and PR_A is the packet delivery ratio for each packet.

In our algorithm, given a required $P_D(X_A)$ from an application, the number of packets for $X_A(n_A)$, and the frame DT, the required packet delivery ratio (PR_A) is estimated and assigned to each packet.

After correlation-aware differential coding is performed, an intra frame becomes an inter frame, resulting in reduced packets but more dependency among frames. Consider the differential coding of frame X_A using the prediction of frame X_B. Suppose X_A becomes frame X'_A after differential coding, and the number of packets in X'_A is reduced to n'_A. To decode frame X'_A at the end user, DT percent of the n'_A packets needs to be successfully decoded. More importantly, its reference frame X_B should also be decoded. Therefore, the probability that X'_A is decodable is given by

$$\begin{aligned} P_D(X'_A) &= P_D(X_B)\cdot\varphi(X'_A) = \varphi(X_B)\cdot\varphi(X'_A) \\ &= \varphi(n_B, \mathrm{DT}, \mathrm{PR}_B)\cdot\varphi(n'_A, \mathrm{DT}, PR'_A) \end{aligned} \quad (30)$$

where n_B and n'_A are the number of packets for X_B and X'_A, and PR_B and PR'_A are their packet delivery ratios.

To maintain the quality of video frames, the decodable probability of a frame after correlation-aware differential coding has to be consistent with that before correlation-aware differential coding. As the decodable probability of a frame is related to the packet delivery ratio (PR) in (28), we need to update the required PR when correlation-aware differential coding is performed. We formulate a problem as follows.

Packet delivery ratio update (PDRU) problem

$$\text{Given: } n_A, n_B, n'_A, \mathrm{DT}, P_D^{\mathrm{req}}(X_A), P_D^{\mathrm{req}}(X_B), p_b \quad (31)$$

$$\text{Find: } \mathrm{PR}_A^{\mathrm{new}}, \mathrm{PR}_B^{\mathrm{new}} \quad (32)$$

$$\text{Maximize: } E\{\eta_c\}$$

$$\text{Subject to :}$$

$$\varphi(n_B, \mathrm{DT}, \mathrm{PR}_B^{\mathrm{new}})\cdot\varphi(n'_A, \mathrm{DT}, \mathrm{PR}_A^{\mathrm{new}}) \geq P_D^{\mathrm{req}}(X_A) \quad (33)$$

$$\varphi(n_B, \mathrm{DT}, \mathrm{PR}_B^{\mathrm{new}}) \geq P_D^{\mathrm{req}}(X_B). \quad (34)$$

If there is no correlation-aware differential coding, for two intra frames X_A and X_B, suppose their required frame decodable probabilities are $P_D^{\mathrm{req}}(X_A)$ and $P_D^{\mathrm{req}}(X_B)$. Given the number of packets in these two frames, n_A and n_B, and the frame DT, based on (29), the required packet delivery ratios for these two frames $\mathrm{PR}_A^{\mathrm{old}}$ and PR_B^{old} can be determined to satisfy the requirements.

After correlation-aware coding, the two frames become the inter frame X'_A and the intra frame X_B. Suppose the required packet delivery ratios for X'_A and X_B are $\mathrm{PR}_A^{\mathrm{new}}$ and $\mathrm{PR}_B^{\mathrm{new}}$, respectively. Based on (29) and (30), the frame decodable probability of X_B is $\varphi(n_B, \mathrm{DT}, \mathrm{PR}_B^{\mathrm{new}})$, and the frame decodable probability of X'_A is $\varphi(n_B, \mathrm{DT}, \mathrm{PR}_B^{\mathrm{new}})\cdot\varphi(n'_A, \mathrm{DT}, \mathrm{PR}_A^{\mathrm{new}})$. The resulting frame decodable probabilities of these two frames should also meet application requirements, which are given as constraints in (33) and (34).

As introduced above, the channel coding rate of a transmission is selected based on reliability requirements and channel condition. When the required reliability is changed, the channel coding rate might need to be updated. Taking into account the effect of channel coding, we introduce a metric called *differential coding efficiency after channel coding* as

$$\eta_c = \frac{\left(\frac{n_B\cdot L}{R^C_{B\_\mathrm{old}}} + \frac{n_A\cdot L}{R^C_{A\_\mathrm{old}}}\right) - \left(\frac{n_B\cdot L}{R^C_{B\_\mathrm{new}}} + \frac{n'_A\cdot L}{R^C_{A\_\mathrm{new}}}\right)}{\frac{n_A\cdot L}{R^C_{A\_\mathrm{old}}}} \quad (35)$$

where $R^C_{A\_\mathrm{old}}$ and $R^C_{B\_\mathrm{old}}$ are the channel coding rates of X_A and X_B, $R^C_{A\_\mathrm{new}}$ and $R^C_{B\_\mathrm{new}}$ are the channel coding rates of X'_A and X_B after correlation-aware coding, and L is the packet length. With a similar form as (3), η_c describes the percentage of saved bits after channel coding.

The objective of the PDRU problem is to maximize $E\{\eta_c\}$ in (32), the average value of η_c for a range of possible SNRs. The problem can be solved as follows. First, we find out the possible combinations of $\mathrm{PR}_A^{\mathrm{new}}$ and $\mathrm{PR}_B^{\mathrm{new}}$ that satisfy constraints (33) and (34). For each possible combination of $\mathrm{PR}_A^{\mathrm{new}}$ and $\mathrm{PR}_B^{\mathrm{new}}$, we obtain the corresponding channel coding rates, $R^C_{A\_\mathrm{new}}$ and $R^C_{B\_\mathrm{new}}$. Specifically, given a certain bit error rate, from a set of predefined channel coding rates, we select the largest channel coding rate that satisfies the required packet delivery ratio $(\mathrm{PR}_A^{\mathrm{new}})$. After $R^C_{A\_\mathrm{new}}$ and $R^C_{B\_\mathrm{new}}$ are estimated, the differential coding efficiency after channel coding in (35) could be determined for this specific bit error rate. We assume that the distribution of possible bit error rates (denoted by p_b) are known in advance, so that the average gain $E\{\eta_c\}$ can be calculated. The solution to this problem will be the required packet delivery ratios $\mathrm{PR}_A^{\mathrm{new}}$ and $\mathrm{PR}_B^{\mathrm{new}}$ that result in the largest average gain $E\{\eta_c\}$. These solutions are then used in constraint (18) in the CAQR algorithm.

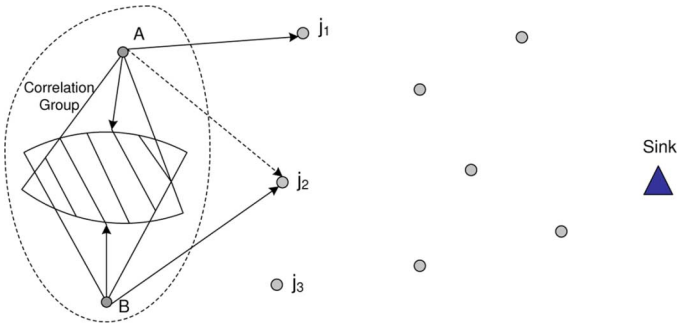

Fig. 3. Correlation-aware load balancing.

3) Correlation-Aware Load Balancing: For flows from the same correlation group that cannot be further compressed, the presence of traffic congestion becomes evident in that video sensors from the same correlation group tend to report the same event and generate traffic concurrently. We introduce a correlation-aware load balancing operation to split these flows to different paths, so that the probability of network congestion could be reduced. As shown in Fig. 3, two sensors in a correlation group share large overlapped FoVs; however, the differential coding gain is low according to our correlation model. As they are likely to generate large amounts of traffic concurrently, we can try to split the flows from the two sensors to different paths.

To achieve correlation-aware load balancing, each node keeps a list of source nodes and their corresponding group IDs that it has generated or routed in a recent period. Suppose node i wants to find a next hop for a flow generated by node V_{id} at group $\mathcal{G}(V_{\text{id}})$. Its candidate neighbor, node j, has a list of source nodes of the flows that it has routed in a recent period, denoted by $(\mathcal{L}\{v^j\})$. Each source node v^j in the list is associated with its correlation group ID $\mathcal{G}(v^j)$. Node j periodically exchanges this list with its neighbors, so that node i is aware of it. For the current flow generated by V_{id}, node i can check if node j has routed flows for other nodes in the same correlation group.

We define a variable x_{v^j} to indicate if a source node v^j is in the same group as V_{id}, which is given by

$$x_{v^j} = \begin{cases} 1, & \text{if } \mathcal{G}(v^j) = \mathcal{G}(V_{id}) \text{ and } v^j \neq V_{\text{id}} \\ 0, & \text{otherwise.} \end{cases} \tag{36}$$

The number of nodes in list $\mathcal{L}\{v^j\}$ that are in the same group as V_{id} can be expressed as $\sum_{v^j \in \mathcal{L}\{v^j\}} x_{v^j}$. For load balancing, the algorithm should prefer to choose a next hop node with a smaller $\sum_{v^j \in \mathcal{L}\{v^j\}} x_{v^j}$, which, as indicated in constraint (19), cannot exceed a threshold w. The threshold w can be set to a certain percentage of the average correlation group size of a network. In this way, for flows from the same correlation groups that cannot be further compressed, we can penalize the case that they share the same forwarding node concurrently (e.g., node j_2 in Fig. 3), thereby reducing the possibility of congestion.

D. Protocol Operation

The CAQR algorithm is summarized as follows. When a WVSN is deployed, correlation groups are first constructed as shown in Section IV-A. After that, if a sensor V_A has a video frame X_A to transmit, it encounters two scenarios: 1) If X_A is an inter frame, V_A will send X_A to the sink. 2) If X_A is an intra frame, V_A selects the optimal intermediate node V_{B^*} by solving the DCIS problem in Section IV-B. The QoS constraints for frames X_A and X_{B^*} are set by solving the PDRU problem in Section IV-C2. Otherwise, if no such intermediate node can be found, V_A will send X_A to the sink node. In both scenarios, next-hop nodes are selected using *Algorithm 1* that solves the DCR problem in Section IV-C.

Algorithm 1 is performed as follows. A sensor first finds out all the next hop candidate nodes that satisfy the load balancing constraint in (19). For each candidate node, the largest channel coding rate R_{ij}^C from $\{R_0^C, \ldots, R_N^C\}$ is found such that the reliability constraint (18) can be satisfied. Using this largest channel coding rate, the sensor checks if the local delay constraints (16) and (17) are met. If so, the corresponding energy consumption (15) for this candidate node can be obtained. The candidate node that results in the smallest energy consumption is selected as the next hop node. In cases that no candidate nodes can satisfy all the four constraints, the load balancing constraint (19) could be relaxed by increasing the threshold w by a small amount, so that more nodes in the neighbor set could be considered as next hop candidates.

Algorithm 1: QoS Guaranteed Next-hop Selection

$C_i = \{j | \sum_{v^j \in \mathcal{L}\{v^j\}} x_{v^j} \leq w, j \in \mathcal{F}_i\}$
for $j \in C_i$ **do**
  $R = \{R_{ij}^C | pr_{ij} \geq \text{PR}_{ij}, R_{ij}^C \in \{R_0^C, \ldots, R_N^C\}\}$
  if $R \neq \emptyset$ **then**
   Find $\{R_{ij}^{C*}\} = \max\{R_{ij}^C \in R\}$
   s.t. $(L)/(R \cdot R_{ij}^C) + \overline{t_{ij}^q} < T_{ij}$
  $(\gamma)/(1-\gamma)(\Delta t_{ij}^q)^2 \leq (T_{ij} - (L)/(R \cdot R_{ij}^C) - \overline{t_{ij}^q})^2$
  end if
end for
$j^* = \arg\min_{j \in C_i} E(L/R_{ij}^C, d_{ij})$

E. Discussion

We now study the resource requirements and complexity for each component of the CAQR algorithm. The correlation groups construction operation is performed just once during the initial deployment of the network; therefore, it does not require any cost during the operation of a network.

For intermediate node selection, a sensor node solves the DCIS problem. Suppose the number of sensor nodes in a correlation group is $N_{\mathcal{G}}$. A sensor finds one node with the largest gain in the group, so the computational complexity is $O(N_{\mathcal{G}})$. The sensor then sends a short message notifying the intermediate node, resulting in $O(1)$ message complexity.

Each sensor solves the distributed next-hop selection problem in Algorithm 1. From a group of forwarding neighbors, it chooses one node as the next hop and also finds the channel coding rate. Suppose the maximum degree of nodes in the network is Δ, and the total number of channel coding rates is N_C. The worst case computational complexity for this problem is $O(\Delta \cdot N_C)$. A node makes decision of the next hop using only local information. Each node periodically broadcast a message to its neighbors, which contains the mean and variance of delay and the estimated channel status on its link. The message complexity is $O(\Delta)$. This type of message exchange is natural for distributed routing protocols for sensor networks. Several representative routing protocols such as [13] and [9] also involve similar communication cost. We estimate that the

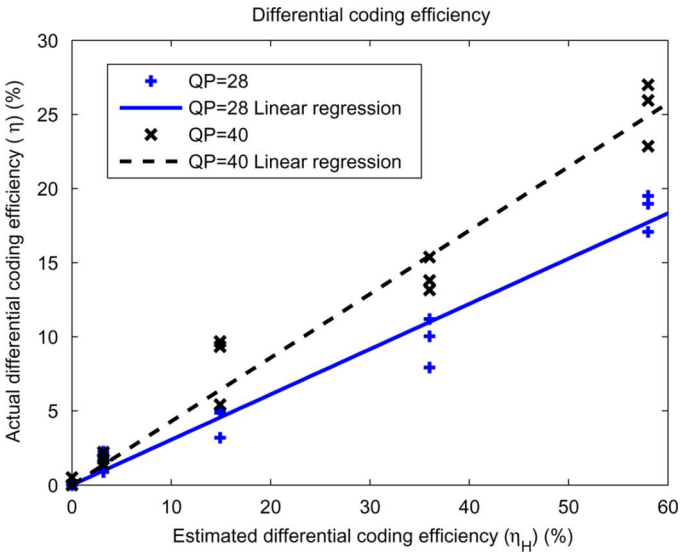

Fig. 4. Estimation of differential coding efficiency.

message exchange complexity of the proposed algorithm is in the same scale as that in [9].

V. Performance Evaluation

We first evaluate the validity of coding efficiency prediction. Then, we test the performance of the proposed routing algorithm through extensive simulations.

A. Coding Efficiency Prediction

We deploy two cameras in a field and record their FoV parameters. The cameras' sensing radius is 30 meters and the offset angle is 60 degrees. By varying the locations and sensing directions of the two cameras, different degrees of correlation can be obtained, resulting in different values of the estimated coding efficiency (η_H) in (4). Each camera captures one image at each deployment. We employ the H.264 Multi-View Coding (MVC) scheme (JMVC 2.5 [1]) to perform differential coding on the two correlated images, and from the resulting rate the actual coding efficiency (η_H) is obtained. Comparisons of η_H and η values are shown in Fig. 4. Different values of estimated differential coding efficiency η_H are obtained, and for each η_H, 3 different groups of images are used for differential coding. The coding rates are obtained under two quantization steps (QP $=$ 28 and 40).

According to the data points in Fig. 4, if given the same prediction of η_H, we find that a larger quantization step results in larger values of actual coding efficiency. Since larger quantization steps allow for more distortion, they may have more bit savings for differential coding. When the quantization step is fixed, the actual coding efficiency (η) is approximately proportional to the predicted coding efficiency (η_H). Therefore, the actual differential coding efficiency η can be predicted by a linear function of η_H, given by

$$\eta = k \cdot \eta_H \tag{37}$$

where k is a ratio that depends on the performance of specific encoding parameters (e.g., quantization step). By performing linear regression, we find that $k = 0.31$ for QP $= 28$ and $k = 0.43$ for QP $= 40$. The average absolute error for this prediction method is 0.01 and the worst case error is 0.03. This linear relationship between the predicted results and experimental performance validates the applicability of the proposed coding efficiency prediction method.

B. Coding Efficiency in QoS Routing

We now evaluate the gain of correlation-aware coding when it is implemented in the QoS routing algorithm. We find solutions to the packet delivery ratio update (PDRU) problem in Section IV-C, and then we test the best average differential coding efficiency after channel coding in (35).

The parameters in the PDRU problem (32) are determined as follows. The average size of an intra frame is determined from the statistics of the video traces in [23]. The payload length of a packet is set to 50 Bytes. The number of packets in a frame can then be estimated from the average size of the frame and the packet length. We use a series of block codes with structures (n, k, t) [17] for dynamic channel coding. The block length is set to 127, and the number of correctable bits t varies from 1 to 31. A single hop scenario with BPSK modulation is considered, where the received SNR is assumed to be uniformly distributed between -5 dB and 15 dB.

The required frame decodable probability (P_D) is assigned by specific applications. We set P_D to three different values here: 0.7, 0.8, and 0.9. The frame decodable threshold DT is related to the error recovering capability of video decoders. Here DT is set to 0.75 and 0.9. We let the original differential coding efficiency η vary from 0 to 0.5, and for each combination of P_D, DT, and η, the PDRU problem is solved and the average differential coding efficiency after channel coding $(E\{\eta_c\})$ is obtained.

Figs. 5 and 6 show $E\{\eta_c\}$ as a function of η. In both figures, a dotted line is plotted as a benchmark line that corresponds to $E\{\eta_c\} = \eta$, which can represent the case of error-free channels. The other lines show the average differential coding efficiency in lossy channel conditions. For different combinations of P_D and DT, the average differential coding efficiency after channel coding is close to the benchmark line. As there is only a little fluctuation of the lossy-channel case compared to the benchmark line, the efficiency of differential coding after channel coding (η_c) could still be approximated by the original differential coding efficiency (η).

C. Correlation-Aware QoS Routing Algorithm

The performance of the proposed routing algorithm is then evaluated using a distributed network simulator in Java. In a field of 100 m $\times$ 100 m, 49 video sensors are deployed in a grid structure, and a sink node is placed in a corner of the field. The sensing directions of the video sensors are uniformly chosen so as to ensure full coverage of the field, and the sensing parameters of the sensors are given in Table I.

The traffic for the video sensors is generated based on the features of WVSN applications. We let a target move in the field according to the Random Waypoint Mobility model where the pause time is set to 0. A video sensor is triggered to capture an image when it detects the target in its FoV. By launching the target from 10 different locations, we can generate 10 sequences of events representing different traffic scenarios. The captured video frames are in QCIF format (176 $\times$ 144), while the size of

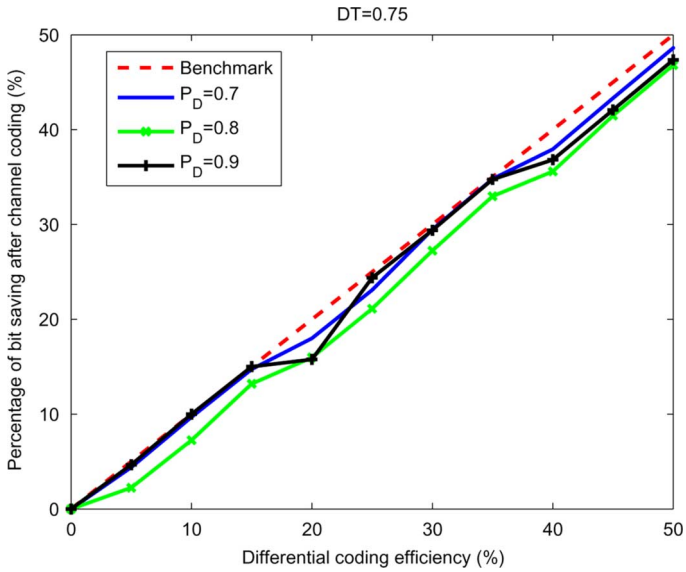

Fig. 5. Differential coding efficiency after channel coding $(\mathrm{DT} = 0.75)$.

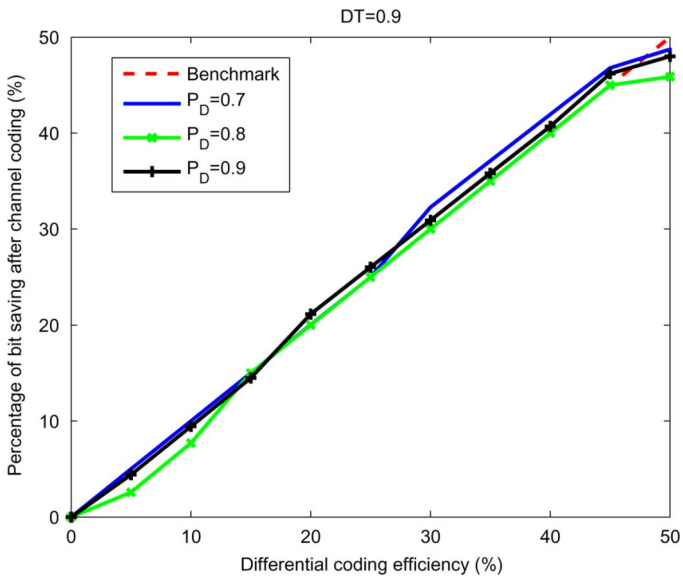

Fig. 6. Differential coding efficiency after channel coding $(\mathrm{DT} = 0.9)$.

an encoded video frame is obtained based on the video traces provided in [23]. If correlation-aware coding is performed, the size of a frame is updated based on the actual coding efficiency in (37).

We use the TDMA scheduling algorithm in [8] as the MAC layer solution. Table II presents the TDMA slot length, transmission range, and rate of each sensor. The parameters for estimating communication and processing energy are also presented. The number of clock cycles (N_{cyc}) for encoding and decoding one QCIF frame is obtained from the results in [12] and [14]. Together with the other parameters in (7) and (8), the communication and processing energy is estimated.

We evaluate the performance of the CAQR algorithm under varying traffic load and QoS requirements. A representative QoS routing algorithm MMSPEED [9] is implemented. We also take the shortest path routing with opportunistic aggregation (SPRO) in [22] as a representative algorithm for bandwidth

TABLE II
PARAMETERS

Offset angle	60°	Sensing radius	30 m
Image size	176×144	Intra period	15
Frame rate	30 fps	DT	0.8
E_{elec}	50 nJ/b	α	2
ε	10 $pJ/b/m^2$	C_{total}	0.67 nF
I_0	1.196 mA	V_T	26 mV
K	239.28 MHz/V	c	0.5 V
N_{cyc} (encoder)	2.3 Mcycles	N_{cyc} (decoder)	0.14 M
Trans. rate	1 Mbps	Trans. range	15 m
Slot length	20 ms		

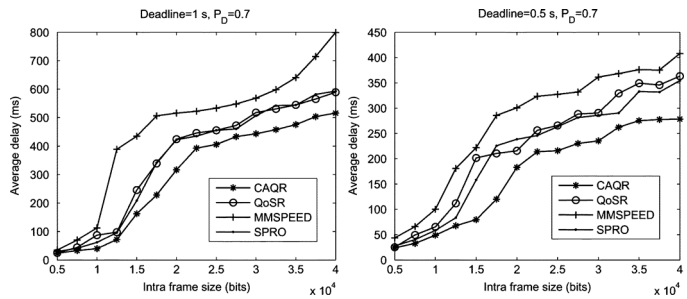

Fig. 7. Average delay.

saving along routing paths. The SPRO algorithm is customized to deliver video traffic: video sensors send their data along paths chosen by shortest path routing, and if a relay node finds that a frame is eligible for compression based on (9), differential coding is performed to save bandwidth. To evaluate the performance of correlation-aware operations, we also compare the CAQR algorithm with QoSR, which is the QoS routing algorithm in Section IV-C without any correlation-aware operations.

We change the amount of traffic injected in the network by varying the source coding rates of the video frames, which is achieved by varying the quantization steps (QP) in the encoder. The range of quantization steps in our simulation is determined by the video quality metric PSNR. Typical values for the PSNR in lossy image and video compression are between 30 and 50 dB. Based on the video traces for QCIF frames in [23], when the PSNR ranges between 30 and 50 dB, the QP ranges between around 16 to 40, and it corresponds to average size of intra frames between 4×10^4 and 0.5×10^4 bits. We also found from the traces [23] that in average the size of an encoded P frame is around 0.2–0.25 times that of an encoded I frame. These statistics are used to set the coding rates in the simulation. For each rate, experiments on the aforementioned 10 different sequences of events are launched, and we measure the average performance of the 10 sequences of events.

Fig. 7 shows the average delay under different source coding rates, with deadline set to 1 s and 0.5 s. In both cases we only consider the delay of packets that are received within the deadline. By exploiting the correlation of video sensors, CAQR reduces the transmission and queueing delays in the network. Therefore, it is seen in Fig. 7 that CAQR results in less average delay than QoSR, the QoS routing algorithm without correlation-aware operations. SPRO introduces shortest path routing and opportunistic compression mechanisms, and it produces similar average delay as that of QoSR. MMSPEED leads to the largest delay among the four algorithms. This is because MMSPEED finds multiple non-shortest paths as long

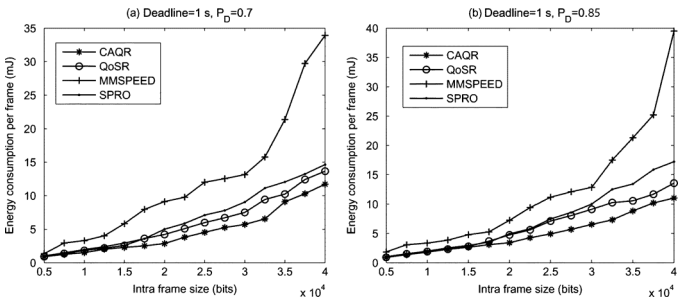

Fig. 8. Average energy consumption per node.

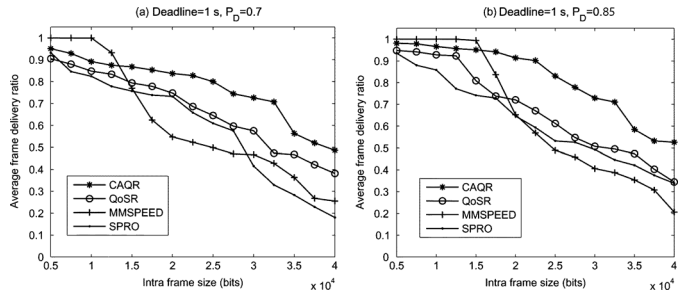

Fig. 9. Frame delivery ratio.

as the delay deadline is met and multi-path transmission brings extra traffic in the network which increases queue lengths.

Next we evaluate the energy efficiency of the proposed algorithm. The total energy consumption consists of the energy for sending and receiving packets and that for processing the video frames. Given the same event, the processing energy for sensing video frames and encoding local video frames will be the same for different routing algorithms, whereas differential coding along routing paths will introduce extra processing energy. Therefore, we just consider the communication energy and the processing energy for differential coding along routing paths. Fig. 8 shows the average energy consumption for one received frame. The proposed algorithm is designed to reduce energy consumption by reducing the transmission of redundant information and selecting energy-efficient next hops. Specifically, through correlation-aware differential coding, CAQR reduces energy consumption by 15% compared to QoSR. And the energy consumption of QoSR is lower than the other two algorithms, which is brought by minimizing energy consumption in next hop selection. SPRO partially reduces the transmission of redundant information in the network, resulting in fewer energy consumption than MMSPEED which does not consider energy consumption in routing decisions.

We now evaluate the quality of received visual information under different reliability requirements. We set the deadline to 1 s, and vary the probability that a video frame is successfully decoded, P_D, to 0.7 and 0.85. For each reported image frame, we count the number of received packets within the deadline. If the percentage of received packets for a frame is above the frame decodable threshold (DT), we deem that it is successfully decoded at the sink. Based on the number of decoded frames, we can obtain the percentage of successfully decoded video frames (frame delivery ratio). Fig. 9 shows the average frame delivery ratio for the 10 sequences of events under different source coding rates. MMSPEED utilizes multi-path forwarding to guarantee reliability. When there is less traffic in the network, MMSPEED produces very good reliability with 100% frame delivery ratio. However, as the traffic in the network increases, MMSPEED suffers from a lot of degradation in frame delivery ratio, in which case the redundancy introduced by multi-path routing is prone to cause congestion in the network. The average frame delivery ratios of SPRO and QoSR are similar. By introducing correlation-aware operations in QoSR, the proposed CAQR algorithm increases the frame delivery ratio by 16% compared to QoSR.

In Figs. 8 and 9, when video frame sizes become larger, i.e., more traffic are injected into the network, there is more gain of the proposed algorithm over the other algorithms in terms of energy consumption and frame delivery ratio. We conclude that exploiting correlation in a video sensor network can enhance network performance, especially when the traffic load is heavy. By incorporating correlation-aware differential coding and load balancing in the routing process, the CAQR algorithm provides an effective way to improve the quality of visual information received at the sink.

VI. Conclusion

We have proposed a correlation-aware QoS routing algorithm for wireless video sensor networks. Based on the correlation characteristics of visual information in sensor networks, we introduce a correlation-aware inter-node differential coding scheme and a correlation-aware load balancing mechanism. These correlation-aware operations are integrated in a distributed routing framework. The whole routing algorithm minimizes energy consumption under delay and reliability constraints. The performance of the algorithm is evaluated in terms of energy efficiency, delay performance, and frame delivery ratio. Evaluation results show that, by integrating correlation-aware operations in the routing process, the proposed algorithm achieves efficient delivery of visual information in wireless video sensor networks.

References

[1] JMVC Reference Software JMVC 2.5. [Online]. Available: http://ftp3.itu.int/av-arch/jvt-site/2008_10_Busan/JVT-AC207.zip.

[2] I. F. Akyildiz, T. Melodia, and K. R. Chowdhury, "A survey on wireless multimedia sensor networks," *Comput. Netw.*, vol. 51, no. 4, pp. 921–960, Mar. 2007.

[3] M. Chen, V. C. M. Leung, S. Mao, and Y. Yuan, "Directional geographical routing for real-time video communications in wireless sensor networks," *Comput. Commun.*, vol. 30, no. 17, pp. 3368–3383, Nov. 2007.

[4] O. Chipara, Z. He, G. Xing, Q. Chen, X. Wang, C. Lu, J. Stankovic, and T. Abdelzaher, "Real-time power-aware routing in sensor networks," in *Proc. 14th IEEE Int. Workshop Quality of Service (IWQoS)*, Jun. 2006, pp. 83–92.

[5] R. Cristescu, B. Beferull-Lozano, and M. Vetterli, "On network correlated data gathering," in *Proc. 23rd Annu. Joint Conf. IEEE Computer and Communications Societies, INFOCOM 2004*, Mar. 2004, pp. 2571–2582.

[6] R. Dai and I. F. Akyildiz, "A spatial correlation model for visual information in wireless multimedia sensor networks," *IEEE Trans. Multimedia*, vol. 11, no. 6, pp. 1148–1159, Oct. 2009.

[7] D. Devarajan, Z. Cheng, and R. Radke, "Calibrating distributed camera networks," *Proc. IEEE*, vol. 96, no. 10, pp. 1625–1639, Oct. 2008.

[8] S. C. Ergen and P. Varaiya, TDMA Scheduling Algorithms for Sensor Networks, Univ. California, Berkley, tech. rep., Jul. 2005.
[9] E. Felemban, C.-G. Lee, and E. Ekici, "MMSPEED: Multipath multi-SPEED protocol for QoS guarantee of reliability and timeliness in wireless sensor networks," *IEEE Trans. Mobile Comput.*, vol. 5, no. 6, pp. 738–754, 2006.
[10] W. Feng, B. Code, E. Kaiser, M. Shea, W. Feng, and L. Bavoil, "Panoptes: Scalable low-power video sensor networking technologies," in *Proc. ACM Multimedia*, Berkeley, CA, Nov. 2003.
[11] B. Girod, A. Aaron, S. Rane, and D. Rebollo-Monedero, "Distributed video coding," *Proc. IEEE*, vol. 93, no. 1, pp. 71–83, Jan. 2005.
[12] K. Goto, A. Hatabu, H. Nishizuka, K. Matsunaga, R. Nakamura, Y. Mochizuki, and T. Miyazaki, "H.264 video encoder implementation on a low-power DSP with low and stable computational complexity," in *Proc. IEEE Workshop Signal Processing Systems Design and Implementation*, Oct. 2006, pp. 101–106.
[13] T. He, J. Stankovic, C. Lu, and T. Abdelzaher, "SPEED: A stateless protocol for real-time communication in sensor networks," in *Proc. 23rd Int. Conf. Distributed Computing Systems (ICDCS)*, May 2003, pp. 46–55.
[14] M. Horowitz, A. Joch, F. Kossentini, and A. Hallapuro, "H.264/AVC baseline profile decoder complexity analysis," *IEEE Trans. Circuits Syst. Video Technol.*, vol. 13, no. 7, pp. 704–716, Jul. 2003.
[15] A. K. Jain, M. N. Murty, and P. J. Flynn, "Data clustering: A review," *ACM Comput. Surv.*, vol. 31, no. 3, pp. 264–323, Sep. 1999.
[16] P. Kulkarni, D. Ganesan, P. Shenoy, and Q. Lu, "Senseye: A multi-tier camera sensor network," in *Proc. ACM Multimedia*, Singapore, Nov. 2005.
[17] S. Lin and D. J. C. Jr, *Error Control Coding: Fundamentals and Applications*. Englewood Cliffs, NJ: Prentice-Hall, 1983.
[18] J. Liu, M. Adler, D. Towsley, and C. Zhang, "On optimal communication cost for gathering correlated data through wireless sensor networks," in *Proc. 12th Annual Int. Conf. Mobile Computing and Networking*, Sep. 2006, pp. 310–321.
[19] Y. Liu, I. Elhanany, and H. Qi, "An energy-efficient QoS-aware media access control protocol for wireless sensor networks," in *Proc. IEEE Int. Conf. Mobile Adhoc and Sensor Systems Conf. (MASS)*, Nov. 2005.
[20] H. Luo, Y. Liu, and S. K. Das, "Routing correlated data with fusion cost in wireless sensor networks," *IEEE Trans. Mobile Comput.*, vol. 5, no. 11, pp. 1620–1632, Nov. 2006.
[21] T. Melodia and I. F. Akyildiz, "Cross-layer quality of service support for UWB wireless multimedia sensor networks," in *Proc. IEEE INFOCOM 2008*, Apr. 2008, pp. 121–125.
[22] S. Pattem, B. Krishnamachari, and R. Govindan, "The impact of spatial correlation on routing with compression in wireless sensor networks," in *Proc. 3rd Int. Symp. Information Processing in Sensor Networks, IPSN 2004*, Apr. 2004, pp. 28–35.
[23] P. Seeling, M. Reisslein, and B. Kulapala, "Network performance evaluation using frame size and quality traces of single-layer and two-layer video: A tutorial," *IEEE Commun. Surv. Tutor.*, vol. 6, no. 3, pp. 58–78, Third Quarter 2004.
[24] S. Soro and W. Heinzelman, "A survey of visual sensor networks," *Adv. Multimedia*, vol. 2009, no. 640386, pp. 1–21, 2009.
[25] A. Vetro, T. Wiegand, and G. J. Sullivan, "Overview of the stereo and multiview video coding extensions of the H.264/MPEG-4 AVC standard," *Proc. IEEE*, vol. 99, no. 4, pp. 626–642, Apr. 2011.
[26] A. Wang and A. Chandrakasan, "Energy-efficient DSPs for wireless sensor networks," *IEEE Signal Process. Mag.*, pp. 68–78, Jul. 2002.
[27] P. Wang, R. Dai, and I. F. Akyildiz, "Collaborative data compression using clustered source coding for wireless multimedia sensor networks," in *Proc. IEEE INFOCOM 2010*, Mar. 2010.
[28] A. Ziviani, B. E. Wolfinger, O. M. B. D. J. F. de Rezende, and S. Fdida, "Joint adoption of QoS schemes for MPEG streams," *Multimedia Tools Appl.*, vol. 26, no. 1, pp. 59–80, May 2005.

Rui Dai (S'08) received the B.S. and M.S. degrees in electrical and computer engineering from Huazhong University of Science and Technology (HUST), Wuhan, China, in 2004 and 2007, respectively, and the Ph.D. degree in electrical and computer engineering in 2011, after working as a graduate research assistant at the Broadband Wireless Networking Laboratory, School of Electrical and Computer Engineering, Georgia Institute of Technology, Atlanta, GA.

Her research interests include wireless sensor networks, multimedia communications, and sensor signal processing for rehabilitation engineering.

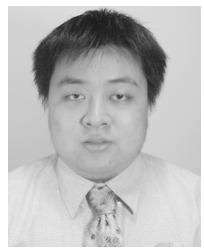

Pu Wang (S'10) received the B.S. degree in electrical engineering from the Beijing Institute of Technology, Beijing, China, in 2003 and the M.Eng. degree in computer engineering from the Memorial University of Newfoundland, St. Johns, NL, Canada, in 2008. He is currently pursuing the Ph.D. degree in electrical engineering under the supervision of Prof. I. F. Akyildiz.

Currently, he is a graduate research assistant in Broadband Wireless Networking Laboratory (BWN Lab), School of Electrical and Computer Engineering, Georgia Institute of Technology, Atlanta, GA. His research interests include wireless sensor networks and mobile ad-hoc networks.

Ian F. Akyildiz (M'86–SM'89–F'96) received the B.S., M.S., and Ph.D. degrees in computer engineering from the University of Erlangen-Nuernberg, Germany, Erlangen, Germany, in 1978, 1981 and 1984, respectively.

Currently, he is the Ken Byers Distinguished Chair Professor with the School of Electrical and Computer Engineering, Georgia Institute of Technology, Atlanta, GA. Since June 2008, he has been an Honorary Professor with the School of Electrical Engineering at the Universitat Politecnico de Catalunya, Barcelona, Spain. His current research interests are in cognitive radio networks, wireless sensor networks, and nano-communication networks.

Prof. Akyildiz is the Editor-in-Chief of *Computer Networks (COMNET) Journal* as well as the founding Editor-in-Chief of the *Ad Hoc Networks Journal* and *Physical Communication Journal*, all with Elsevier. He received numerous awards, including the 1997 IEEE Leonard G. Abraham Prize Award (IEEE Communications Society) for his paper entitled "Multimedia group synchronization protocols for integrated services architectures" published in the IEEE JOURNAL ON SELECTED AREAS IN COMMUNICATIONS in January 1996; the 2002 IEEE Harry M. Goode Memorial Award (IEEE Computer Society) with the citation "for significant and pioneering contributions to advanced architectures and protocols for wireless and satellite networking"; the 2003 IEEE Best Tutorial Award (IEEE Communication Society) for his paper entitled "A survey on sensor networks," published in IEEE COMMUNICATIONS magazine, in August 2002; the 2003 ACM Sigmobile Outstanding Contribution Award with the citation "for pioneering contributions in the area of mobility and resource management for wireless communication networks"; the 2004 Georgia Tech Faculty Research Author Award for his "outstanding record of publications of papers between 1999–2003"; the 2005 Distinguished Faculty Achievement Award from School of ECE, Georgia Tech; the 2009 Georgia Tech Outstanding Doctoral Thesis Advisor Award for his more than 20 years of service and dedication to Georgia Tech and producing outstanding Ph.D. students; and the 2009 ECE Distinguished Mentor Award from School of ECE, Georgia Tech. He has been a Fellow of the Association for Computing Machinery (ACM) since 1996.